

Piezo-QEXAFS with fluorescence detection: fast time-resolved investigations of dilute specimens

Dirk Lützenkirchen-Hecht,* Sven Grundmann and Ronald Frahm

Institut für Materialwissenschaft und Institut für Experimentalphysik, Fachbereich 8, Bergische Universität-Gesamthochschule Wuppertal, Gausstrasse 20, 42097 Wuppertal, Germany. E-mail: dirklh@uni-wuppertal.de

First X-ray absorption spectroscopy experiments with a vibrating piezo-driven double-crystal monochromator (piezo-QEXAFS) and fluorescence detection are reported. It is shown that high-quality XANES spectra can be recorded on a time scale of about 50 ms per spectrum, even for very low concentrations of $<10 \text{ mmol l}^{-1}$ using fluorescence detection. The quality of the spectra, possible applications, as well as present limits of the technique will be discussed.

Keywords: XAFS; QEXAFS; fluorescence detection; diluted specimens; time-resolved studies.

1. Introduction

Time-resolved X-ray absorption spectroscopy is an invaluable tool for the investigation of the dynamical behaviour of many physical, chemical and biological processes and has widely been used to study, for example, phase transformations, crystallization, nucleation and growth phenomena, decomposition and combustion reactions or solid-state transformations (see, for example, Guay *et al.*, 1991; Frahm *et al.*, 1992; Als-Nielsen *et al.*, 1995; Rumpf *et al.*, 1999; Ressler *et al.*, 2000). Both the quick-scanning EXAFS (QEXAFS) technique and the dispersive EXAFS (DEXAFS) method can be applied for such investigations. In the QEXAFS mode, overheads associated with all movements of a double-crystal monochromator on a point-by-point basis are eliminated by scanning the spectrum continuously, thus measuring the spectrum on-the-fly within a couple of seconds (Frahm, 1989), while the dispersive EXAFS method employs a curved polychromator crystal and parallel data acquisition with a position-sensitive detector (Matsushita & Kaminaga, 1980; Phizackerley *et al.*, 1983; Hagelstein *et al.*, 1989), enabling time-resolved studies on a milliseconds time scale. However, DEXAFS investigations are restricted to transmission experiments, and cannot make use of fluorescence detection in an efficient way, which is, on the other hand, essential for the investigation of diluted specimen such as biological systems or those samples which cannot be penetrated by X-rays (*e.g.* thick samples). In contrast to the DEXAFS technique, the experimental details of a QEXAFS set-up are very similar to a standard EXAFS spectrometer so that all important detection methods such as electron or ion yield detection (Kakar *et al.*, 1997), reflectivity

(Hecht *et al.*, 1996) or fluorescence detection (Frahm *et al.*, 1991, 1992) have been successfully applied for a large number of time-resolved experiments. In any case, it should be mentioned that DEXAFS experiments using sequential data acquisition with a time resolution of about 50 ms for an XANES spectrum and fluorescence detection have been reported recently (Pascarelli *et al.*, 1999).

Recently, a time resolution of less than 10 ms per spectrum was achieved for concentrated samples in a QEXAFS experiment which utilizes a piezo-driven vibrating double-crystal monochromator (piezo-QEXAFS; Bornebusch *et al.*, 1999). For these experiments the monochromator crystals were mounted on piezo-driven tilt tables which can be actuated by sinusoidal voltages with frequencies of more than 100 Hz, resulting in very fast near-edge energy scans upwards and downwards. Thus, two spectra are recorded per period. So far, mainly transmission measurements have been performed. In this contribution, we will report on the first fluorescence piezo-QEXAFS experiments.

2. Experimental

The experiments described here were performed at the X-ray undulator beamline BW1 (Frahm *et al.*, 1995) at the DORIS III storage ring at HASYLAB (DESY, Hamburg) operating at a positron energy of 4.45 GeV with $\sim 50\text{--}140 \text{ mA}$ of stored current. A fixed-exit double-crystal monochromator with two flat Si(111) crystals was used. The accessible scan range of the monochromator in the piezo-QEXAFS mode is limited by the piezo tilt stages, which enable changes in the Bragg angles of the monochromator crystals of up to about 0.13° , corresponding to a scan range of $\sim 50\text{--}100 \text{ eV}$ at a photon energy of about $7\text{--}10 \text{ keV}$ (Bornebusch, 1998). Therefore, piezo-QEXAFS measurements enable the very fast acquisition of near-edge data (Bornebusch *et al.*, 1999). For the present study, N_2 -filled ionization chambers were used as detectors for the incoming and transmitted intensities. A windowless large-area Si (pin) photodiode (AXUV 300, International Radiation Detectors Inc., Torrance, USA) with an active area of approximately 330 mm^2 and suitable filter foils detect the fluorescence radiation. Pin photodiodes have proven their applicability for EXAFS experiments in a series of previous investigations due to their high efficiency, excellent linearity, low noise, wide dynamic range and simple electronics (see, for example, Bouldin *et al.*, 1987; Storb *et al.*, 1991; Lengeler *et al.*, 1991; Dalba *et al.*, 1996). The readout of the programmable Keithley 428 current amplifiers was performed by means of a high-speed ADC board (DATEL PCI-416M2 with four individual 16-bit ADCs on board, 16-bit resolution, up to 200 kHz sampling rate) and a fast personal computer (Bornebusch, 1998; Grundmann, 1999). Further experimental details of the piezo-QEXAFS technique are given elsewhere (Frahm, 1995; Lützenkirchen-Hecht *et al.*, 2001). High-purity metal foils (Cu, Ni, Au, Ta) as well as GeO_2 powder were investigated as reference samples in transmission and fluorescence. CuSO_4 solutions were prepared from analytically pure substances and

deionized water. They were investigated in a cell consisting of a Teflon frame and large Kapton windows.

3. Results and discussion

In Fig. 1, $\ln(I_1/I_2)$ transmission spectra of a copper metal foil at the Cu *K*-edge are presented together with the simultaneously measured fluorescence XAFS data I_F/I_1 (9.1 Hz oscillation frequency corresponding to 55 ms per spectrum). The ADC rate was 50 kHz. In each case, 20 subsequent 'up' spectra are plotted. The high quality of the raw fluorescence data, *i.e.* the low noise level and the high reproducibility as well as the effect of self absorption in the Cu sample of thickness $\sim 7 \mu\text{m}$ (corresponding to approximately two absorption lengths), are clearly visible. For the further data evaluation of the measured piezo-XANES spectra, the noise contributions were determined similar to the procedure described by Dent and co-workers (Dent *et al.*, 1992). A mean spectrum of all the data points was calculated, smoothed by a Fourier-filtering technique and subtracted from the raw fluorescence data in order to separate the noise from the signal. The results show that the mean noise averaged over a single scan is about 0.40% of the signal corresponding to a signal-to-noise (S/N) level of about 250 for the fluorescence data of the Cu foil. For comparison, the related value determined from piezo-QEXAFS data

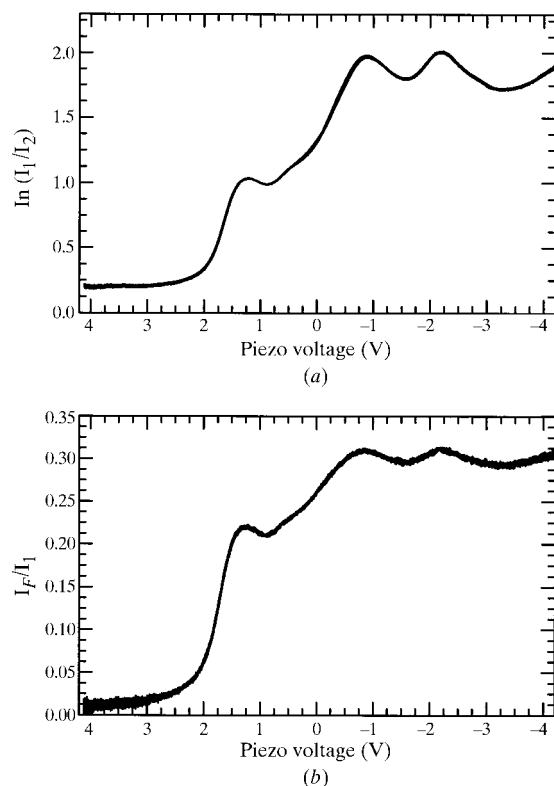


Figure 1

Raw piezo-QEXAFS (Cu *K*-edge, 9.1 Hz, 55 ms per spectrum, 50 kHz ADC rate) of a Cu-metal foil (thickness $6.8 \mu\text{m}$) measured in (a) transmission and (b) fluorescence. Twenty subsequently measured 'up' spectra are shown.

measured in transmission is about 0.22% corresponding to $S/N \simeq 450$, which again illustrates the high data quality which is available with piezo-QEXAFS. It should be mentioned that similar results regarding the quality of the fluorescence data were obtained for Ni and Au metal foils and concentrated ($\sim 100 \text{ mmol l}^{-1}$) CuSO_4 solutions with S/N ratios of the order of 200.

A closer inspection of the measured fluorescence data generally shows that the noise level increases slightly at the end points of the scans. This observation can be related to the intensity I_1 which is transmitted by the monochromator as a function of the piezo-voltage as follows. For moderately high frequencies below the first resonance of the piezo tilt tables, which is about 17 Hz, I_1 is almost constant and not dependent on the piezo-voltage over a large voltage range. However, a certain decrease in I_1 is always observed at the reversal points of the spectra, *i.e.* the parallelism of both monochromator crystal surfaces is perturbed when the piezo tilt tables with the monochromator crystals change the direction of their motion. The resulting decrease in transmitted intensity can easily explain the increased noise observed in the end points of the piezo-QEXAFS fluorescence spectra. A more detailed investigation of the frequency-dependent synchronization of the

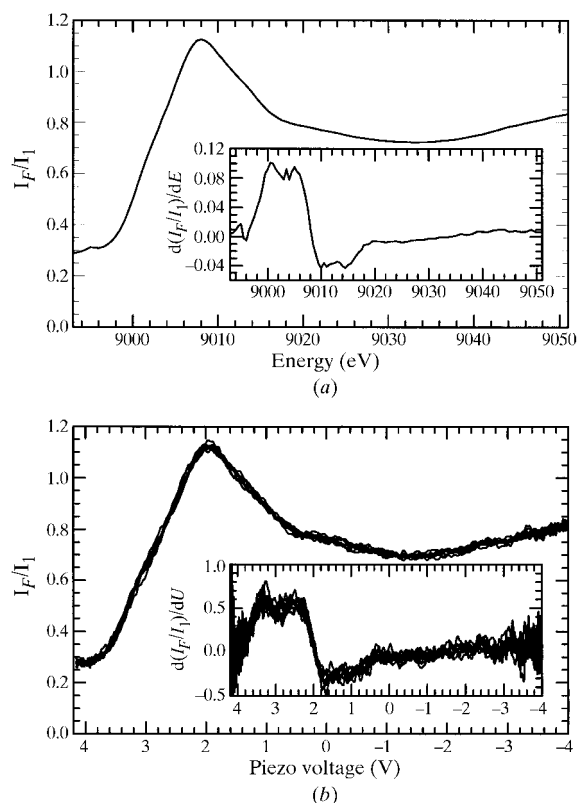


Figure 2

(a) EXAFS step-scan of a 10 mmol l^{-1} CuSO_4 solution measured in fluorescence at the Cu *K*-edge in about 12 min. The insert depicts the derivative spectrum. (b) Piezo-QEXAFS (Cu *K*-edge, 9.1 Hz, 55 ms per spectrum) of a 10 mmol l^{-1} CuSO_4 solution measured in fluorescence mode. Ten subsequent 'up' spectra are displayed. The insert depicts the related derivative spectra.

monochromator crystal movements is currently under preparation (Lützenkirchen-Hecht *et al.*, 2001).

In Fig. 2, raw fluorescence piezo-QEXAFS data I_F/I_1 (9.1 Hz piezo-frequency, 55 ms per spectrum) measured at the Cu *K*-edge of diluted aqueous CuSO_4 solutions are presented for a Cu concentration of 10 mmol l^{-1} . This concentration corresponds to an atomic concentration of about 180 p.p.m. The data are compared with a conventional step-scan measured in about 12 min. Obviously, the white-line intensity at $\sim 9009 \text{ eV}$ photon energy corresponding to a piezo-voltage of $\sim 2 \text{ V}$ as well as the edge jump are identical for both measurements. The S/N ratio determined as described above is about 80 for the fluorescence piezo-QEXAFS data, *i.e.* it is significantly lowered compared with the measurements of metal foils or concentrated CuSO_4 solutions (100 mmol l^{-1}). In the latter case, a S/N ratio of more than 180 was determined. However, even weak structures in the absorption spectrum can be reproduced by the fast piezo-XANES measurements. This can be more clearly seen by comparison of the derivative spectra of the step-scan with the piezo-QEXAFS spectra, which are presented in the inserts of Fig. 2(a) and 2(b). The double-peaked maximum in the step-scan data between 9000 eV and 9005 eV and the two minima between 9010 eV and 9015 eV are well reproduced by the piezo-QEXAFS data (peaks between 3.4 V and 2.5 V, and 1.5 V and 0.7 V piezo-voltage, respectively). It has to be mentioned that the absolute values of both sets of derivative data cannot be compared due to the different normalization during the calculation of the derivatives; *i.e.* the conversion factor from the photon energy scale to the piezo-voltage scale has to be taken into account. However, the intensity ratios of the high- and low-energy features are very similar, *i.e.* $0.09/-0.04 \simeq 2.2$ compared with $0.6/-0.25 \simeq 2.4$.

In Fig. 3, raw fluorescence piezo-QEXAFS data obtained from a 2.5 mmol l^{-1} CuSO_4 solution corresponding to an atomic concentration of $\sim 45 \text{ p.p.m. Cu}$ are presented. Ten

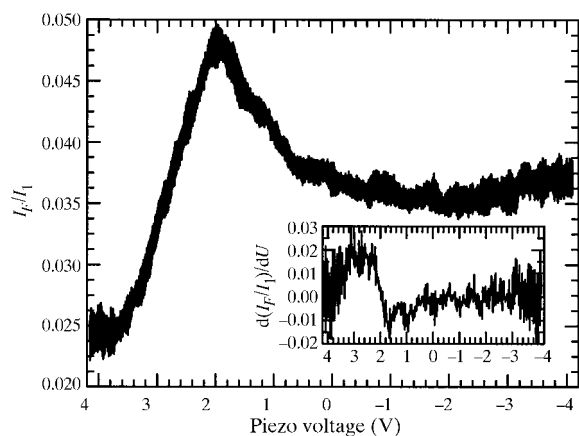


Figure 3

Raw fluorescence piezo-QEXAFS (Cu *K*-edge, 9 Hz, 55 ms per spectrum, 50 kHz ADC rate) of a diluted CuSO_4 solution with a concentration of 2.5 mmol l^{-1} . Ten subsequent 'up' spectra are shown. The insert depicts the average of the derivative spectrum (see text for more details).

subsequent 'up' spectra, each measured in 55 ms with an ADC rate of 50 kHz, are shown. The reduced edge jump as well as an increased noise in the data are prerequisites of the lowered concentration. We determined a S/N ratio of about 60–65. This can also be seen in the derivative fluorescence spectrum, which was calculated from the average of the ten spectra shown. Similar to the step-scan and piezo-QEXAFS measurements of the 10 mmol l^{-1} CuSO_4 solution (Fig. 2), however, the most characteristic features of CuSO_4 could be clearly resolved in the averaged data. Therefore, XANES investigations of real samples of such low concentrations are possible with a time resolution in the subsecond range.

For concentrations below 1 mmol l^{-1} , the edge is still visible in the piezo-QEXAFS spectra; however the fluorescence data became very noisy and detailed features of the absorption data could not be resolved in the raw data. For example, for fluorescence piezo-QEXAFS data (9.1 Hz, 55 ms per spectrum) from a $800 \mu\text{mol l}^{-1}$ CuSO_4 solution corresponding to about 15 p.p.m. atomic Cu concentration, we determined a signal-to-noise ratio of less than 50. Nevertheless, in the derivative spectrum obtained by averaging over 10–15 subsequent 'up' or 'down' spectra, broad features corresponding to those of CuSO_4 could be detected. Averaging over longer periods of time can still improve the data quality. In conclusion, at the wiggler beamline BW1 at HASYLAB, a concentration of about 2 mmol l^{-1} corresponding to about 40 p.p.m. seems to be the current detection limit for XANES investigations of diluted samples using the piezo-QEXAFS technique with fluorescence detection and a time resolution in the subsecond range.

4. Conclusions

We have shown that piezo-QEXAFS in combination with fluorescence detection is a well suited tool for time-resolved X-ray absorption spectroscopy of concentrated and diluted specimen in the hard X-ray energy range. The results show that high-quality fluorescence data with signal-to-noise ratios of more than 200 and a time resolution of $\sim 50 \text{ ms}$ per spectrum can be obtained for concentrated specimens. For the investigation of diluted samples with absorber concentrations of ~ 50 – 100 p.p.m. , an averaging procedure over five to ten spectra seems to be necessary to achieve XANES data of acceptable quality, leading to an accordingly reduced time resolution. This time resolution is comparable with that which was recently achieved with dispersive optics and sequential fluorescence data acquisition for a sample containing 1 wt% Ge in a BN matrix (Pascarelli *et al.*, 1999). However, one should keep in mind that these experiments were performed at a third-generation synchrotron source and with a high-photon-flux insertion device.

Due to the fact that piezo-QEXAFS experiments in the transmission geometry have been performed with appreciable higher frequencies of more than 100 Hz, it can be concluded that the mechanical stability of the monochromator is not limiting the time resolution or the sensitivity of the piezo-QEXAFS experiments with fluorescence detection. Currently,

the photon flux is limiting the attainable S/N ratios of the fluorescence data. A higher photon flux thus should enable investigations of more dilute systems and push the accessible time resolution towards some few milliseconds.

For the future, time-resolved investigations of biochemical reactions involving, for example, metalloproteins in low concentrations are planned using the piezo-QEXAFS technique with fluorescence detection. In addition, the application of the method for *in situ* studies of catalysts with active metal species such as Cu or Zn in low concentrations is under consideration. Furthermore, it is planned to use piezo-QEXAFS with fluorescence detection for the investigation of self-propagating high-temperature synthesis reactions (see, for example, Frahm *et al.*, 1992).

We gratefully acknowledge financial support by the BMBF (grant No. 05SU8PF1) and the MSWWF, Nordrhein-Westfalen. Additional support was supplied by HASYLAB. We would like to thank M. Richwin, A. Krämer and P. Keil for their invaluable help at the beamline.

References

- Als-Nielsen, J., Grübel, G. & Clausen, B. S. (1995). *Nucl. Instrum. Methods*, **B97**, 522–525.
- Bouldin, C. E., Forman, R. A. & Bell, M. I. (1987). *Rev. Sci. Instrum.* **58**, 1891–1894.
- Bornebusch, H. (1998). Diploma thesis, Heinrich-Heine-Universität Düsseldorf, Germany. (In German.)
- Bornebusch, H., Clausen, B. S., Steffensen, G., Lützenkirchen-Hecht, D. & Frahm, R. (1999). *J. Synchrotron Rad.* **6**, 209–211.
- Dalba, G., Fornasini, P., Soldo, Y. & Rocca F. (1996). *J. Synchrotron Rad.* **3**, 213–219.
- Dent, A. J., Stephenson, P. C. & Greaves, G. N. (1992). *Rev. Sci. Instrum.* **63**, 856–858.
- Frahm, R. (1989). *Rev. Sci. Instrum.* **60**, 2515–2518.
- Frahm, R. (1995). *Synchrotron Rad. News*, **8**(2), 38.
- Frahm, R., Barbee, T. W. Jr & Warburton, W. (1991). *Phys. Rev. B*, **44**, 2822–2825.
- Frahm, R., Weigelt, J., Meyer, G. & Materlik, G. (1995). *Rev. Sci. Instrum.* **66**, 1677–1680.
- Frahm, R., Wong, J., Holt, J. B., Larson, E. M., Rupp, B. & Waide, P. A. (1992). *Phys. Rev. B*, **46**, 9205–9208.
- Grundmann, S. (1999). Diploma thesis, Heinrich-Heine-Universität Düsseldorf, Germany. (In German.)
- Guay, D., Tourillon, G., Dartyge, E., Fontaine, A. & Tolentino, H. (1991). *J. Electrochem. Soc.* **138**, 399–405.
- Hagelstein, M., Cunis, S., Frahm, R., Niemann, W. & Rabe, P. (1989). *Physica B*, **158**, 324–325.
- Hecht, D., Frahm, R. & Strehblow, H.-H. (1996). *J. Phys. Chem.* **100**, 10831–10833.
- Kakar, S., Björneholm, O., Weigelt, J., de Castro, A. R. B., Tröger, L., Frahm, R., Möller, T., Knop, A. & Rühl, E. (1997). *Phys. Rev. Lett.* **78**, 1675–1678.
- Lengeler, B., Dedek, U. & Storb, C. (1991). *Mater. Sci. Forum*, **79**, 389–395.
- Lützenkirchen-Hecht, D., Grundmann, S. & Frahm, R. (2001). *J. Synchrotron Rad.* In preparation.
- Matsushita, T. & Kaminaga, U. (1980). *Jpn. J. Appl. Cryst.* **13**, 465–472.
- Pascarelli, S., Neisius, T. & De Panfilis, S. (1999). *J. Synchrotron Rad.* **6**, 1044–1050.
- Phizackerley, R. P., Rek, Z. U., Stephenson, G. B., Conradson, S. D., Hodgson, K. O., Matsushita, T. & Oyanagi, H. (1983). *J. Appl. Cryst.* **16**, 220–232.
- Ressler, T., Timpe, O., Neisius, T., Find, J., Mestl, G., Dieterle, M. & Schlögl, R. (2000). *J. Catalysis*, **191**, 75–85.
- Rumpf, H., Hormes, J., Möller, A. & Meyer, G. (1999). *J. Synchrotron Rad.* **6**, 468–470.
- Storb, C., Dedek, U., Weber, W. & Lengeler, B. (1991). *Nucl. Instrum. Methods Phys. Res. A*, **306**, 544–548.